

## APPLIED SAMPLING METHODOLOGY AND ANALYSIS OF NONLINEAR ACOUSTIC PROPERTIES IN SOLIDS OF REVOLUTION

**G.I. Ivanov**  
Sofia High School of Mathematics (Bulgaria)

**Abstract.** The main focus of this work is the research of the resulting sound caused by a constant airflow through the open end of a bottle by varying the relevant parameters. For a more in depth analysis, additional experiments with test tubes are carried out. The study aims to describe and document the influence of the parameters experimentally and with the help of theoretical apparatus, some of which are: Form, shape and material of the bottle, properties of the gas, filling agent. The aforementioned variables are defined and sorted on the basis of their effect on the process. Unpredicted acoustic properties emerge when the shape of the bottle is varied significantly. New methods for physical data collection such as an AFS (Acoustic Feedback System) and SRP (Solids of Revolution Parameterization) are introduced and compared to the already existing ones, in order to better equate for the emergent acoustic properties. For a holistic evaluation various samples and relations from the well-described acoustic properties are tested against their contemporary physical description for their predictive power. Similar methods are introduced to the analysis of the previously undescribed acoustic phenomena and presented with a multi-layered approach for full comparison.

**Keywords:** acoustic feedback system; airflow system; solid of revolution; resonance; Helmholtz resonance; standing wave

### 1. Introduction

The contemporary theoretical modelling fails to account for the full spectral range of the acoustic feedback from a tested system. Present approximations, such as “Helmholtz Resonance” and “Standing Wave Resonance”, are ubiquitously applied, yet are not enough to describe emergent acoustic phenomena. The methodology of acoustic excitation is crucial for the accurate data gathering and minimization of external influences, foreign to the acoustic system. All of the aforementioned observations are fundamental to the motivations of conducting this research.

### 2. Experimental Setup

Two methods for data collection are described. The results from the systems will be compared in the section “Experimental Results”, labelled for their respective or-

igin (AS/AFS). In both instances the sound is recorded and analysed with the audio editing software “Audacity”. For setup one the signal transformations are carried out by the software and for AFS - done as described in section “Background”.

## 2.1 Airflow System (AS)

An SR (Solid of Revolution) and a stationary microphone are positioned with the space between them a constant - 0,5 m. This provides consistency in the data, which allows for their simultaneous application as a basis for comparison; For minimizing the fluctuations of the speed of air, the airflow is supplied with a hot air gun at a constant setting of 30 C; The basic mechanism is that of “Acoustic Excitation”, where the resonant modes are respectively excited and produce a descriptive frequency.

## 2.2 Acoustic Feedback System (AFS)

This method for data acquisition was developed for minimizing external and background noise and focuses on the acoustic feedback, given by the system. The SR is positioned above a speaker and under a microphone (Fig.1). A sweep signal (Linear-Frequency Chirp) with time-domain function:

$$x(t) = \sin \left[ \phi_0 + 2\pi \left( \frac{c}{2}t^2 + f_0 t \right) \right]$$

is introduced in the system, where the feedback is then reinforced for a multi-layered approach. This method entails the continuous damping or amplification of the frequencies that are respectively foreign or natural to the system. The current analysis focuses only on feedback of rank 1 (first-time response of the system). Future experiments will be extensively dedicated on higher-order feedback.

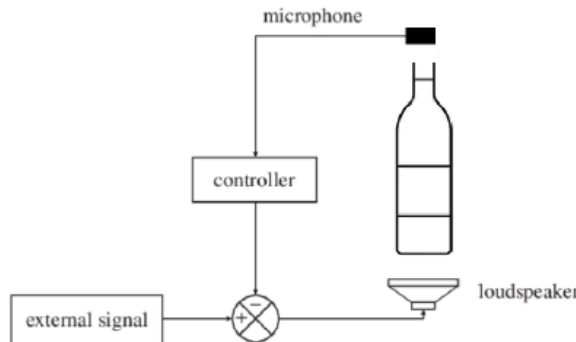


Fig. 1: AFS

## 3. Background

Section “Background” is focused on the signal analysis and the existing theoretical models, which in turn are reviewed for their respective assumptions and func-

tional range. Novel parameterizations for the description of the physical bodies are introduced and evaluated.

### 3.1 Resonance

A specific section, dedicated to the topic of resonance, is required for clearing up the reason behind the phenomenon and validating the newly introduced experimental setup (AFS): A phenomenon of resonance is observed when the frequency of a forced vibration approaches the natural frequency of the system and in the process is amplified. The mechanism of occurrence is the transfer of energy between two or more different modes. The mechanism of an AFS utilizes this phenomenon in the process of looping the feedback from the acoustic system - The continuous damping of the foreign frequency to the system, coupled with the amplification of the natural resonant modes leads to obtaining a clear spectrum of the acoustic properties of a given SR.

### 3.2 Signal Analysis

In order the audio signal to be processed and used as data a few transformations are required. The audio signal is recorded in small samples, making the setup a discrete-time system (Fig.6). The given data points are obtained from the DAQ Setup (Data Acquisition).

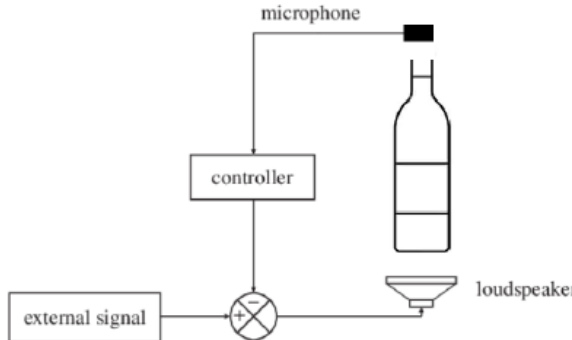


**Fig. 2:** Sampl Signal

The type of signal that an AFS works with is periodic - the excited air column resonates, which fundamentally presupposes a recurrent oscillation (It is important to mention that the different resonant modes have). For a periodic signal the following relation is true:

$$x[n + N] = x[n]$$

Where  $N$  is the minimum integer for which the relation holds and is called a period. We define energy of the signal as:

$$\mathcal{E} = \sum_{n=-\infty}^{+\infty} |x[n]|^2$$

A periodic signal has infinite energy over  $n = (-\infty, +\infty)$ , but the average power over  $n = (-\infty, +\infty)$  is finite and equal to the power, calculated over a single period:

$$\mathcal{P} = \frac{1}{N} \sum_{n=0}^{N-1} |x[n]|^2$$

Any discrete-time signal can be expressed as a sum of scaled and delayed impulses

$$x[n] = \sum_{k=-\infty}^{+\infty} x[k] \delta[n - k] = \sum_{k=-\infty}^{+\infty} x[n - k] \delta[k]$$

When applied to the physical context relation (2) becomes the functional dependence of the sound pressure ( $p$ ) to the moment of time ( $t$ ):

$$p[t + T_0] = p[t]$$

When we are working with complex systems such as the acoustic properties of SRs, the resonant modes of the system become many and hard to theoretically model. Nonetheless from the properties of mechanic waves in an ideal gas, we also know that the sound pressure at a given time of ( $t$ ) is equal to the sum of the partial sound pressures from the different resonant modes, so relation (5) becomes:

$$p(t) = \sum_{n=1}^N p_n(t)$$

Where every  $p_n$  is some acoustic oscillation:

$$p_n(t) = A_n \cos(\omega_n t - \phi_n) = \operatorname{Re} \{ \hat{p}_n e^{-i\omega_n t} \}$$

And (7) becomes (9) which clearly fits the formula for DFT (Discrete Fourier Transform) (10):

$$p(t) = \sum_{n=-\infty}^{n=\infty} \hat{q}_n e^{-i\omega_n t} = \operatorname{Re} \left( \sum_{n=0}^{\infty} \hat{p}_n e^{-i\omega_n t} \right)$$

$$X_k = \sum_{n=0}^{N-1} x_n e^{-i2\pi kn/N}$$

We can redefine the energy definition (3) in relation to the given time series:

$$E = \int_{-\infty}^{\infty} |x(t)|^2 dt$$

The aforementioned relation (11) is equal to the sum of the square of its FT (Fourier Transform) as follows from the *Parseval's Theorem*:

$$E = \int_{-\infty}^{\infty} |x(t)|^2 dt = \int_{-\infty}^{\infty} |\hat{x}(f)|^2 df$$

Where the  $\hat{x}(f)$  is the already familiar transform in relation to the time-series (and  $w = 2\pi f$ ):

$$\hat{x}(f) = \int_{-\infty}^{\infty} e^{-2\pi ift} x(t) dt$$

Since the integral on the right-hand side of (12) is the energy of the signal, the integrand  $|\hat{x}(f)|^2$  can be interpreted as a density function describing the energy per unit frequency contained in the signal at the frequency  $f$ . In light of this, the energy spectral density of a signal  $x(t)$  is defined as:

$$S_{xx}(f) = |\hat{x}(f)|^2$$

The same transformations can be done for the power of the given signal in relation to the time series:

And following the same process as for the *Energy Spectral Density* we can de-

$$P = \lim_{T \rightarrow \infty} \frac{1}{T} \int_0^T |x(t)|^2 dt$$

rive the final expression:

$$S_{xx}(\omega) = \lim_{T \rightarrow \infty} \mathbf{E} [|\hat{x}(\omega)|^2]$$

To put this in the physical context - the equivalent physical signal in relation to the time series is that of the sound pressure  $p(t)$ :

$$[p^2(t)]_{\text{av}} = [p(t)p^*(t)]_{\text{av}} = \sum_{n=-\infty}^{\infty} \sum_{m=-\infty}^{\infty} \hat{q}_n \hat{q}_m^* \left( e^{-i(\omega_n - \omega_m)t} \right)_{\text{av}} = \sum_{n=-\infty}^{\infty} |\hat{q}_n|^2$$

Therefore the spectral density function  $p_f^2(f)$  is:

$$p_f^2(f) = \lim_{(\Delta f)_b \rightarrow 0} \left\{ \frac{(p_b^2)_{av}}{(\Delta f)_b} \right\}$$

Where  $(p_b^2)_{av}/(\Delta f)_b$  is the average contribution per unit bandwidth to the mean squared acoustic pressure, which in turn gives us the contribution to  $(p^2)_{av}$  from a band of frequencies between  $f_1$  and  $f_2$ :

$$(p_b^2)_{av} = \int_{f_1}^{f_2} p_f^2(f) df$$

Following from the aforementioned transformations we can then deduce the resulting *sound-pressure spectrum level* from (19) by using the definition for *dB* representation:

$$L_{ps}(f) = 10 \log \left( \frac{p_f^2(f)(\Delta f)_{ref}}{p_{ref}^2} \right) \approx 10 \log \left( \frac{(p_b^2)_{av} (\Delta f)_{ref}/(\Delta f)_b}{p_{ref}^2} \right)$$

Which in turn for our theoretical basis can be adapted simply as:

$$L_p = 10 \log \left( \frac{(p_s^2)_{av}}{p_{ref}^2} \right)$$

The aforementioned transformations are applied to the signal to acquire the training data for the machine learning solutions. Due to the required vectorization of the given data points, a few manual transformations are done in order to have the necessary format. For example, physically the most adequate representation of the data in relation to the fundamental frequency  $f_a$  would deem  $p_{ref} = p_f$ . The problem is that this transformation would make the maximum value of  $(L_p)_{max} = 0$  and the rest of the values of  $L_p < 0$  without a particular limit. For this reason, the best way is to scale down the spectrum to one that is represented by values of  $L_p^* \in (0; 1)$  - This is done by formulating the new  $L_{p_i}^*$  in the following way:

This in turn will allow for the analysis in section "Parameter Correlation" with parameter  $a$ .

### 3.3 Existing Models

There are several existing models describing the acoustic properties of the oscillating air within a cavity, based on its form. The problem is that despite the accurate results in their functional range, they are still highly limited in their predictive

power for the whole spectrum. This section is split into two parts dedicated respectively to each model and focuses on finding the border cases and their reason for emergence. Particular corrections to the definitions of the parameters are applied - a thorough explanation is present in the subsection “Experimental correction”. Each of the models is used for the description of a particular phenomenon. For clarity purposes at the point of application the reasoning behind it is cleared.

The described models are:

### 3.3.1 Helmholtz Resonance

The original experiment is carried out with a specifically created object that is spherical and has a great relative difference between the radius of the cross section of the open end and the widest part, as seen from (Fig.4). This allows for modelling the movement of the air as a separate oscillation of a mass ( $m$ ), where the rest of the volume acts as a spring. The speed with which the process happens is high, which then allows us to assume that the process is adiabatic (the system is thermally insulated):

$$f = \frac{c}{2\pi} \sqrt{\frac{S}{VL}}$$

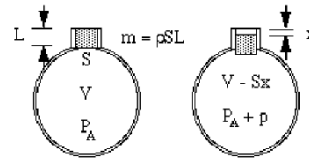


Fig. 4: Air Oscillation

Where  $c$  is the speed of sound,  $S$  and  $L$  are the cross section and the length of the neck respectively, and  $V$  is the volume of the cavity. With this model we can make the following observations:

The shape has to be spherical with a clearly-defined neck.

The cavity is functionally described with just 3 parameters - *Volume*, *Length of neck* and *Area of the open end*. This entails a very big variation in the plausible shape, when describing a particular SR (Solid of Revolution).

### 3.3.2 Experimental Correction

Throughout the experiments a certain trend can be seen. By just using the Helmholtz model (1) the theoretically predicted frequencies are a lot higher than the recorded values. It is estimated that a correction is necessary. The conventional definition of the neck is the cylinder on the top of the volume. From our experiments this proved to be a fairly inaccurate estimation. The newly defined value can be empirically deduced from the following functional relations:

$$L_{\text{eff}} = \left( \frac{c}{2\pi f_{\text{exp}}} \right)^2 \frac{A}{V}$$

This can be then tested by changing the apparent volume of the cavity with some value of

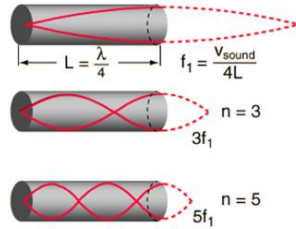
$$\left[ \frac{c^2}{4\pi^2 A} \right] T_i^2 = L_{\text{eff}} (V_o - \Delta V_i)$$

After an empirical examination a claim can be made of the physical background for such a difference in  $L_{\text{eff}}$  - The air volume is active in  $L$  equal to the distance between the open end and the widest point of the SR. Fig (4) shows a table with some of the corrected values.

Some of the corrected values							
Bottle	C1	B12	Z1	V1	Q1	Q2	B1
$L$ [cm]	5,6	4,6	8,9	10,1	5,9	8,1	6,1
$L_c$ [cm]	1,2	2,2	2	5,2	1,7	1,5	1,6

### 3.3.3 Standing Wave

In the case of the aforementioned model the subject of study is the oscillation of an air column within a cylinder. The expression describing the process has several variations. In the context of this work only two are used - a cylinder open at both ends and a cylinder open at one end. In this model there are clearly defined nodes (zero displacement) and anti-nodes (maximum displacement). This entails the presence of secondary harmonic oscillations because of the possibility to fit different patterns of air column displacements that fulfil the conditions.



**Open at both ends (2.1)** - as it is discussed later, this applies to the harmonic oscillations of the air within the neck of the SR (if present). In the equation  $n$  is the number of the harmonic oscillation ( $n = 1$  is the fundamental frequency) and can have the value of any integer ( $n = 1, 2, 3 \dots n$ ). An illustration can be found in the "Appendix".

$$f = \frac{c}{\lambda_n} = \frac{nc}{4L}$$

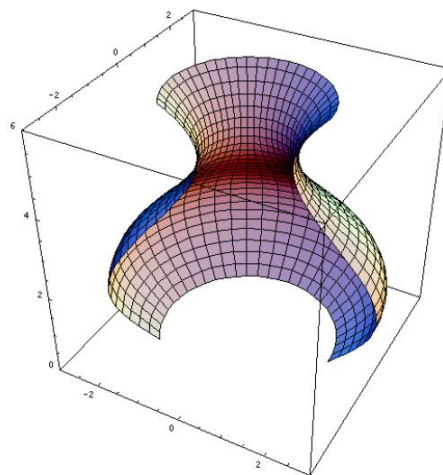
**Open at one end (2.2)** - this describes the oscillation of the air column within a cylinder with one open end and as it is later seen, it also applies to any SR with one

open end. In the equation  $n$  is the number of the harmonic oscillation ( $n = 1$  is the fundamental frequency) and can have the value of any odd integer ( $n = 1, 3, 5 \dots n$ ).

$$f = \frac{c}{\lambda_n} = \frac{nc}{2L}$$

### 3.4 Solids of Revolution Parameterization

As it is seen in the “Analysis” section the familiar parameterization of  $V, L, H$  and  $S$  is useful for determining particular frequencies, but is far from enough to describe the full acoustic properties, some of which are very important for their various applications. For this reason a new parameterization is introduced, in order to fully describe the given properties of the system. If we follow this line of reasoning the best parameterization of an object/cavity would be a 3-D render. The problem with such a method of course is that it is very resource-draining and experimentally hard to determine. This creates the need for a more optimal, but still an accurate estimation of the given shape. For this reason the *Solids of Revolution Parameterization* is introduced. Thus far all experiments are carried out with bodies that fit the description of a **SR** that is a shape that can be represented mathematically as the integral of a particular curve around the axis of symmetry:



Where the volume of the SR can be represented with the following expression:

$$V = \pi \int_a^b f(x)^2 dx$$

A similar method of discrete sampling (in the section *Signal Analysis*) needs to be introduced in order for the parameterization to serve as input data. For this reason a process of sampling the SRs is created, where different shapes and dimensions are represented with the same sample size. The process of sampling goes through outlining the silhouette of the SR from a photo and then sampling equidistant points.

This method allows for customization and modulation of the sample size - an optimization can be made based on the preferred goal - accuracy or resource efficiency. On the x-axis the coordinates vary from 0 (at the base of the SR) to  $h$ , which is respectively the height of the SR. In our case the dimensions of [x] = meters for optimization purposes - as such every  $x_i \in (0; 1)$   $x_i \in (0; 1)$ , for every tested SR is under 1 m in height. If necessary for the application redefinitions of the dimensions can easily be made.

A sample point is  $A_i(x_i; y_i)$ , following the relation of  $x_i = kd_{max}$ ;  $y_i = \frac{ih}{N}$ , where  $k \in (0; 1]$  and  $i \in (0; N]$ . The data follows to be represented in a matrix, where:

$$A = \begin{pmatrix} a_{11} & a_{12} \\ \vdots & \vdots \\ a_{n1} & a_{n2} \end{pmatrix} = \begin{pmatrix} x_1 & y_1 \\ \vdots & \vdots \\ x_n & y_n \end{pmatrix}$$

A point is  $A_i(x_i; y_i)$ , following the relation of  $x_i = kd_{max}$ ;  $y_i = \frac{ih}{N}$  (for equidistant sampling, where  $k \in (0; 1]$  and  $i \in (0; N]$ ). After vectorization for the use as input data, we get :

$$A' = \begin{pmatrix} x_1 \\ \vdots \\ x_n \\ y_1 \\ \vdots \\ y_n \end{pmatrix}$$

#### 4. Experimental results & Analysis

This section is dedicated to the experimental results from the 2 acoustic systems - AS & AFS and their analysis using the different methods, presented in section *Background*. The main focus is the evaluation of the produced data and the review of the achieved results with the various models. A few methods of increasing substantially the size of the datasets are discussed in the subsections *Volume & Length of the neck*

##### 4.1 Methods for increasing the size of the datasets

The main problem with collecting physical data is that it is highly inefficient and almost impossible to do experiments with 1000+ bottles in order to

achieve a sufficient database to make any claims onto the validity of the data. For that reason the following two methods are presented in order to tackle the fundamental problem we have with physical systems. Two ways to increase substantially the given datasets is by varying the acoustic properties of a single SR. By applying them we can achieve a highly increased efficiency in the data we can gather from using only one SR. That is possible by displacing the air within the cavity with a form of a medium, which does not itself change the acoustic properties other than with its own volume (as it can be seen in the subsection *Filling agent*). Another form of variation is discussed in subsection *Length of the neck*, where by respectively elongating the neck of the given cavity, the acoustic properties change themselves. The aforementioned methods are used in order to produce more training data - this allows for more than  $100 \times 10$  acoustic variations per SR.

#### 4.1.1 Volume

In this subsection water is used as a filling medium to the acoustic cavity. The air that previously filled the SR is displaced, and thus directly changing the volume that influences the process (described through the physical terms of the Helmholtz model (1) - a change in the air that acts as a spring). The reason behind using water as a filling medium rather than other variants is examined in the subsection “*Filling agent*”. As it can be seen in the charts bellow, with just one SR a lot of sample sizes can be achieved by simply displacing the air in the acoustic cavity.

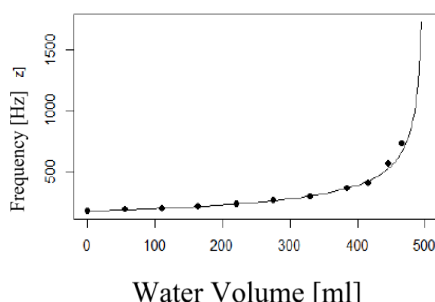


Fig. 12: SR Z1

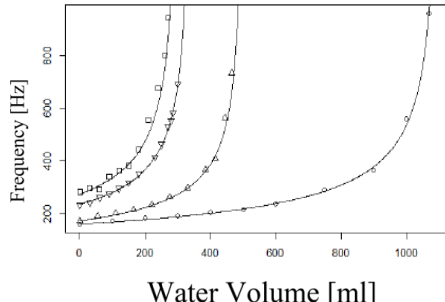


Fig. 13: □-C1; ▽-B1 ; △-Z1 ; ○-B12

#### 4.1.2 Filling Agent

The way that the volume is displaced is by using some kind of a filling agent. This section proves that the effect the filling agent has on the acoustic properties is just with its effective volume. The following experiments are done by adding glycerol to the system - a fluid that is a lot more dense and viscous than water and yet the results are within the range of error.

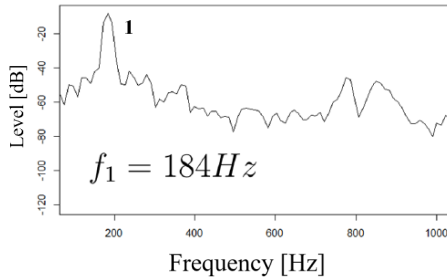


Fig. 14: Bottle Z1 - Water 55ml

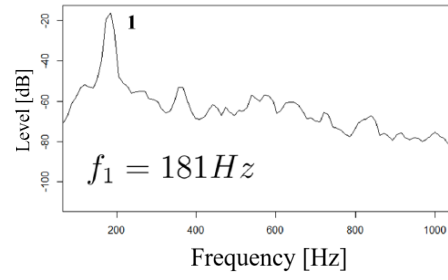


Fig. 15: Bottle Z1 - Glycerol 55ml

#### 4.1.3 Length of the neck

By simply elongating the open end of the SRs a lot more sampling data can be achieved. The physical basis of this method is the increase in the travelled distance by the air (Model (1) - Helmholtz).

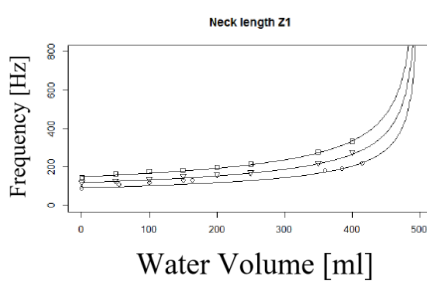
Fig. 16:  $\square$ - $L+3\text{cm}$ ;  $\triangledown$ - $L+10\text{cm}$ ;  $\circ$ - $L+23\text{cm}$ ;

Fig. 17: SR Z1

#### 4.2 AS Experimental Results & Theoretical Models

This section is focused on reviewing the data from the first experimental setup (AS). Observations will be made on what parameters affect this particular system and the validity of the results.

## Properties of Data

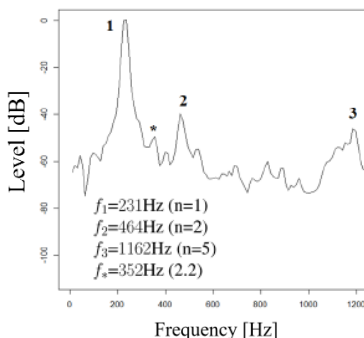


Fig. 18: SR C1

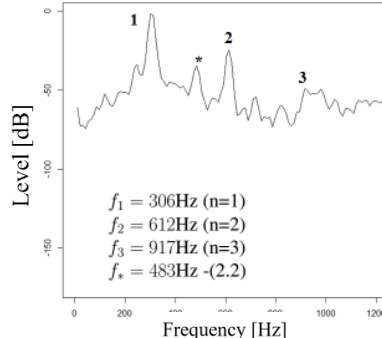


Fig. 19: SR Q2

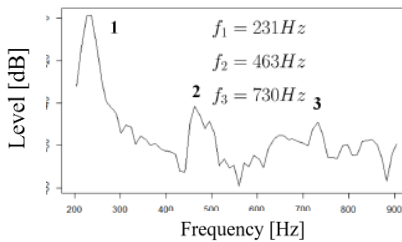


Fig. 20: SR Q1

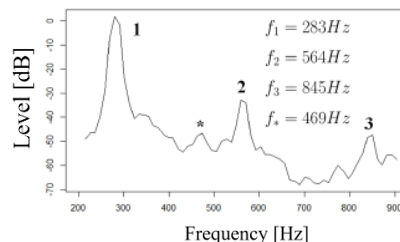


Fig. 21: SR B1

From all for the presented spectra can be observed various frequency peaks and disturbances. To all of them there are recurrent patterns between the various frequencies that can easily be deduced as the secondary oscillations to the system. Average accuracy per noted peak on the table is **94%**.

### 4.3 AFS Experimental Setup & Data Analysis

On the table below are depicted the initial input signal (AF1) and the respective acoustic response, given by the system for SR B1. Basing our reasoning on the physical phenomenon of *Resonance* described in the subsection from *Background* with the same name, we can claim that every peak, resting above the line of (AF1) is that of a resonant mode due to the observed amplification.

## Properties of Data

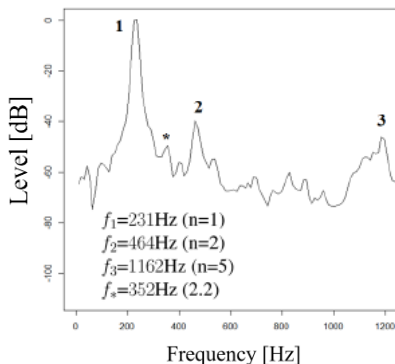


Fig. 18: SR C1

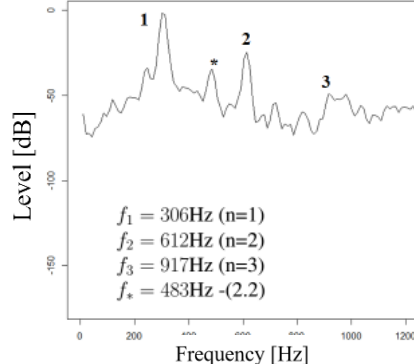


Fig. 19: SR Q2

Using the AFS method we are to expect a greater accuracy due to the elimination of a lot of the background noise and errors from the program. This can be seen from the slight increase in accuracy of **98%** for the applied models at the peaks.

### 5. Transitional Forms

In the case of some bottles there are emergent acoustic properties that are not described by the aforementioned models. On Fig. 19, 20, 21 и 22 there are particular peaks that are different than the fundamental frequency. After a short analysis the main peaks can be attributed to the secondary harmonic oscillations of the air within the neck of the bottle ( $f_1, f_2, f_3$ ). A more interesting observation is the presence of peak  $f_*$ . After a comparison it can be seen that the value of that frequency corresponds to the resonant one in a cylinder that is open at one end and has the height of the investigated bottle. From those observations a conclusion can be made about the actual resonance in the bottle and it is the fact that the air oscillates with simultaneously with different frequencies. For some bottles the peak  $f_*$  is not that pronounced (the loudness is lower). A possible reason behind this phenomenon can be attributed to the shape of the bottle, which is studied in the following section.

### 6. Shape

The hypothesis that is tested in this section assumes that the shape determines the ratio between the loudness of the peaks from the two models. In the expression of the Helmholtz resonance there are 3 defining parameters. Those values do not serve as a sufficient condition to unambiguously depict the shape of the bottle. It is possible that for the same values of those 3 parameters, there could be significant

variation in its contour. In subsections “Relation between the two models” and “Parametric correlation” a method for testing the influence of the shape is laid out.

### 6.1 Correlation between the two models

For the hypothesis to be a valid claim (that the shape of the bottle is what determines the emergent properties). The ratio between the two peaks ( $f_1$ ;  $f_2$ ) has to stay a constant. On Fig.23 the ratio between the loudnesses is plotted against the time. The ratio stays fixed, which then allows us to make the claim that it is dependent on the shape of the bottle.

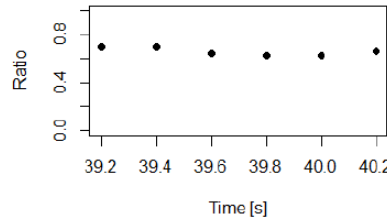


Fig. 22: Ratio for bottle Q2

### 6.2 Parametric Correlation

The parameter, investigated in this subsection, is  $\alpha = \frac{R_w}{R}$ , where  $R_w$  is the radius at the widest section from the bottle and  $R$  is the radius at open end. Hypothetically a cylinder would have an  $\alpha = 1$ . By definition the Helmholtz model has a neck, a lot smaller than the acoustic cavity. For this reason it is to be expected that  $\alpha_h$  is a lot smaller than one ( $\alpha_h \ll 1$ ). In the ideal case the ratio between the loudness of the two peaks would approach infinity, as  $\alpha$  approaches 1:  $\lim_{\alpha \rightarrow 1} \frac{L_{f^*}}{L_{f^1}} = \infty$  (Because in a cylinder there is no Helmholtz resonance).

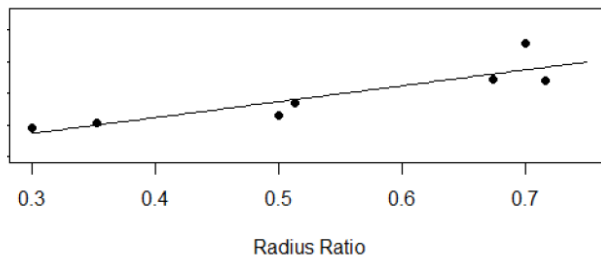


Fig. 23: Parametric correlation

On Fig.24 there is a positive correlation, so the graph suggests a relationship between the parameter  $a$  and the formation of the 2 models. As it is evident, the loudness of the frequency from (2.2) increases while the fundamental frequency (1) decreases. This proves that the shape has an influence, undocumented before. It is important to note that the relationship is not linear. What is seen is the local derivative of the function. Methods with which the relationship could be found are proposed in subsection “Analysis for future optimization”.

## 7. Applications

The project is structured in such a way, that every section has a personal contribution and an application for it, which in turn can be used independently or simultaneously with the other. The main focuses are:

**Acoustic Feedback System (AFS)** - The construction of the AFS allowed for full optimization of the produced data and an empirical way of determining the acoustic modes. The applications fall in various fields like *music instrument tuning, spatial mapping, metal vapour lasers and more*. The mechanism of \Positive Feedback is used in various resonant systems, reaching further than even the field of acoustics.

**Solids of Revolution Parameterization (SRP)** - This is a method of transforming 3-D symmetric objects into matrix form with different sample sizes and then be utilized for various algorithms and forthcoming theoretical models. Its application falls in the fields of *nonlinear and spatial acoustics, as well as acoustic-tracing*.

## 8. Educational Value

The general setup of the experiment provides and inexpensive and efficient way of studying fundamental concepts in acoustics. The study of the corresponding physical modelling can be done on multiple educational levels, making it an accessible and interesting project for high schoolers and students alike. In acoustics the ability to model resonances and spectra without excessive mathematical apparatuses is hard to come by, making this an important introductory experiment into the field. For example, similar versions of the problem have been used in the IYNT and the IYPT, both of which are international tournaments in science for high schoolers. In the case of those competitions, the problem can be developed without using calculus or any university - level math (such is the appeal of the “Helmholtz resonance”). As with any physics problem, the possible development of this experiment does not end with the simple concepts, mentioned in this paper, and provides yet unexplored opportunities for research.

## 9. Concluding Remarks

The contemporary theoretical modelling fails to account for the full spectral range of the acoustic feedback from the tested system. This project focused on developing different methods for solving that problem by introducing more effective

empirical and sampling methods (namely AFS & SRP). There are indications in the effectiveness of the newly-introduced AFS and SRP methods: The developed signal transformations and experimental setup are what is to prove crucial in the following analysis and experiments.

## REFERENCES

Epperlein, J.P. & Bamieh, B. (2012). *A Frequency Domain Method for Optimal Periodic Control*. American Control Conference

Burgess, J.C. (1991). Chirp design for acoustic system identification. *J. Acoust. Soc. Am.* 91 (3)

Forsell, U. & Ljung, L. (1998). *Closed-loop identification revisited*, Automatica 35

Illingworth, S. J., Morgans, A. S. & Rowley, C. W. (2011). Feedback control of flow resonances using balanced reduced-order models. *Journal of Sound and Vibration* 330

 **G.I. Ivanov**  
Sofia High School of Mathematics  
61, Iskar St.  
Sofia 1000, Bulgaria  
E-mail: info@smg.bg